

# Anomalous $WW\gamma$ Vertex in $\gamma p$ Collision

S. Atağ\* and İ.T. Çakır

Ankara University Department of Physics

Faculty of Sciences, 06100 Tandogan, Ankara, Turkey

The potential of LC+HERAp based  $\gamma p$  collider to probe  $WW\gamma$  vertex is presented through the discussion of sensitivity to anomalous couplings and  $p_T$  distribution of the final quark. The limits of  $-0.04 < \Delta\kappa < 0.04$ ,  $-0.11 < \lambda < 0.11$ , at 95% C.L. can be reached with integrated luminosity  $200pb^{-1}$ . The limit for  $\Delta\kappa$  is comparable to one which is expected from LHC. The bounds are also obtained from corresponding ep collider using Weizsäcker-Williams Approximation to compare with real photons.

## I. INTRODUCTION

Recently there have been intensive studies to test the deviations from the Standard Model (SM) at present and future colliders. The investigation of three gauge boson couplings plays an important role to manifest the non abelian gauge symmetry in standard electroweak theory. The precision measurement of the triple vector boson vertices will be the crucial test of the structure of the SM.

It is known that present collider measurements at LEP2 [1] and Tevatron [2] can not probe anomalous triple gauge boson self couplings to precision better than  $O(10^{-1})$ . Further analyses of  $WW\gamma$  vertex has been given by several papers for ep collider HERA [3–8], projected future colliders LHC [9] and linear electron-positron collider (LC) [10]. After LC is constructed  $\gamma e$ ,  $\gamma\gamma$ , linac-ring type  $ep$  and  $\gamma p$  modes should be discussed and may work as complementary to basic colliders. The Linear Collider design at DESY [10,11] is the only one that can be converted into an ep [12,13] collider.  $\gamma p$  collider mode is an additional advantage of this linac-ring type ep collider [14,15] where real gamma beam is obtained by the Compton backscattering of laser photons off linear electron beam. Estimations show that the luminosity for  $\gamma p$  collision turns out to be of the same order as the one for ep collision due to the fact that  $\sigma_p \gg \sigma_\gamma$  where  $\sigma_p$  and  $\sigma_\gamma$  are transverse sizes of proton and photon bunches at collision point. Since most of the photons are produced at high energy region in the Compton backscattering the cross sections are about one order of magnitude larger than parental ep collider for photoproduction processes. According to present project at DESY 500 GeV electrons from linear electron beam are allowed to collide 820 GeV protons from HERA ring [12,13]. Parameters of this LC+HERAp and its  $\gamma p$  option are shown in Table I [14]. Therefore such kind of high energy  $\gamma p$  colliders will possibly give additional information to linac-ring type ep colliders for a variety of processes [15,16]. In this paper we examine the potential of future LC+HERAp based  $\gamma p$  collider to probe anomalous  $WW\gamma$  coupling and compare the results with those from its basic ep collider and other projected future colliders.

TABLE I. Main parameters of LC+HERAp based ep and  $\gamma p$  colliders.

Machine	$\sqrt{s_{ep}}$ TeV	$\sqrt{s_{\gamma p}^{max}}$ TeV	$L_{ep} \simeq L_{\gamma p} (cm^{-1} s^{-1})$
LC+HERAp	1.28	1.16	$1 \times 10^{31}$

Corresponding author: Fax:+90 312 2232395, e-mail: atag@science.ankara.edu.tr

## II. LAGRANGIAN AND CROSS SECTIONS

C and P parity conserving effective lagrangian for two charged W-boson and one photon interaction can be written following the papers [17,18]

$$L = e(W_{\mu\nu}^\dagger W^\mu A^\nu - W^{\mu\nu} W_\mu^\dagger A_\nu + \kappa W_\mu^\dagger W_\nu A^{\mu\nu} + \frac{\lambda}{M_W^2} W_{\rho\mu}^\dagger W_\nu^\mu A^{\mu\rho}) \quad (1)$$

where

$$W_{\mu\nu} = \partial_\mu W_\nu - \partial_\nu W_\mu$$

and dimensionless parameters  $\kappa$  and  $\lambda$  are related to the magnetic dipol and electric quadrupole moments. For  $\kappa = 1$  and  $\lambda = 0$  Standard Model is restored. In momentum space this has the following form with momenta  $W^+(p_1), W^-(p_2)$  and  $A(p_3)$

$$\begin{aligned} \Gamma_{\mu\nu\rho}(p_1, p_2, p_3) = & e[g_{\mu\nu}(p_1 - p_2 - \frac{\lambda}{M_W^2}[(p_2 \cdot p_3)p_1 - (p_1 \cdot p_3)p_2])_\rho \\ & + g_{\mu\rho}(\kappa p_3 - p_1 + \frac{\lambda}{M_W^2}[(p_2 \cdot p_3)p_1 - (p_1 \cdot p_2)p_3])_\nu \\ & + g_{\nu\rho}(p_2 - \kappa p_3 - \frac{\lambda}{M_W^2}[(p_1 \cdot p_3)p_2 - (p_1 \cdot p_2)p_3])_\mu \\ & + \frac{\lambda}{M_W^2}(p_{2\mu}p_{3\nu}p_{1\rho} - p_{3\mu}p_{1\nu}p_{2\rho})] \end{aligned} \quad (2)$$

where  $p_1 + p_2 + p_3 = 0$ . There are three Feynman diagrams for the subprocess  $\gamma q_i \rightarrow W q_j$  and only t-channel W exchange graph contributes  $WW\gamma$  vertex. One should note that  $\gamma p$  collision isolates  $WW\gamma$  coupling but many processes in  $e^+e^-$ , pp and ep collisions include mixtures of  $WW\gamma$  and  $WWZ$  couplings.

The unpolarized differential cross section for the subprocess  $\gamma q_i \rightarrow W q_j$  can be obtained using helicity amplitudes from [6] summing over the helicities

$$\frac{d\hat{\sigma}}{d\hat{t}} = \frac{2}{\hat{s} - M_W^2} \frac{\beta}{64\pi\hat{s}} \sum_{\lambda_\gamma, \lambda_W} \frac{1}{2} M_{\lambda_\gamma, \lambda_W}^2 \quad (3)$$

where

$$M_{\lambda_\gamma, \lambda_W} = \frac{e^2}{\sqrt{2} \sin\theta_W} \frac{\hat{s}}{\hat{s} + M_W^2} \sqrt{\beta} A_{\lambda_\gamma, \lambda_W}, \quad \beta = 1 - \frac{M_W^2}{\hat{s}} \quad (4)$$

and  $\theta_W$  is the Weinberg angle.

For the signal we are considering a quark jet and on-shell W with leptonic decay mode

$$\gamma p \rightarrow W^\mp + jet \rightarrow \ell + p_T^{miss} + jet, \quad \ell = e, \mu \quad (5)$$

In this mode charged lepton and the quark jet are in general well separated and the signal is in principle free of background of SM.

The total cross section for the subprocess  $\gamma q_i \rightarrow W q_j$  can be divided into two parts, direct, and resolved-photon production

$$\hat{\sigma} = \hat{\sigma}_{dir} + \hat{\sigma}_{res} \quad (6)$$

The direct part is given as follows

$$\begin{aligned} \hat{\sigma} = & \frac{\alpha G_F M_W^2}{\sqrt{2}\hat{s}} |V_{q_i q_j}|^2 \{ (|e_q| - 1)^2 (1 - 2\hat{z} + 2\hat{z}^2) \log\left(\frac{\hat{s} - M_W^2}{\Lambda^2}\right) - [(1 - 2\hat{z} + 2\hat{z}^2) \\ & - 2|e_q|(1 + \kappa + 2\hat{z}^2) + \frac{(1 - \kappa)^2}{4\hat{z}} - \frac{(1 + \kappa)^2}{4}] \log \hat{z} + [(2\kappa + \frac{(1 - \kappa)^2}{16}) \frac{1}{\hat{z}} \\ & + (\frac{1}{2} + \frac{3(1 + |e_q|^2)}{2}) \hat{z} + (1 + \kappa)|e_q| - \frac{(1 - \kappa)^2}{16} + \frac{|e_q|^2}{2}] (1 - \hat{z}) \\ & - \frac{\lambda^2}{4\hat{z}^2} (\hat{z}^2 - 2\hat{z} \log \hat{z} - 1) + \frac{\lambda}{16\hat{z}} (2\kappa + \lambda - 2)[(\hat{z} - 1)(\hat{z} - 9) + 4(\hat{z} + 1) \log \hat{z}] \} \end{aligned} \quad (7)$$

where  $\hat{z} = M_W^2/\hat{s}$  and  $\Lambda^2$  is cut off scale in order to regularize  $\hat{u}$ -pole of the colinear singularity for massless quarks. In the case of massive quarks there is no need such a kind of cut. The resolved-photon production cross section can be calculated using Breit-Wigner formula for  $q_\gamma q_p \rightarrow W$  fusion process

$$\hat{\sigma}(q_i \bar{q}_j \rightarrow W) = \frac{\pi\sqrt{2}}{3} G_F m_W^2 |V_{ij}|^2 \delta(x_i x_j s_{\gamma p} - m_W^2) \quad (8)$$

where  $V_{ij}$  is the Cabibbo-Kobayashi-Maskawa (CKM) matrix. For the integrated cross sections we need parton distribution functions inside the photon and proton. The photon structure function  $f_{q/\gamma}$  consists of perturbative pointlike parts and hadronlike parts. The pointlike part can be calculated in the leading logarithmic approximation and is given by the expression

$$f_{q/\gamma}^{LO}(x, Q_\gamma^2) = \frac{3\alpha e_q^2}{2\pi} [x^2 + (1-x)^2] \log \frac{Q_\gamma^2}{\Lambda^2} \quad (9)$$

where  $e_q$  is the quark charge. For the integrated total cross section over the quark distributions inside the proton, photon and the spectrum of backscattered laser photon the following result can be obtained easily

$$\sigma_{res} = \sigma_0 \int_{m_W^2/s}^{0.83} dx \int_x^{0.83} \frac{dy}{xy} f_{\gamma/e}(y) f_{q_i/p}\left(\frac{m_W^2}{xs}, Q_p\right) [f_{q_j/\gamma}\left(\frac{x}{y}, Q_\gamma^2\right) - f_{q_j/\gamma}^{LO}\left(\frac{x}{y}, Q_\gamma^2\right)] \quad (10)$$

with

$$\sigma_0 = \frac{\pi\sqrt{2}}{3s} G_F m_W^2 |V_{ij}|^2 \quad (11)$$

Since the contribution from the pointlike part of the photon structure function was already taken into account in the calculation of the direct part it was subtracted from  $f_{q/\gamma}(x, Q_\gamma^2)$  in the above formula to avoid double counting on the leading logarithmic level.

In a similar way direct part of the integrated cross section can be obtained

$$\sigma_{dir} = \int_{\tau_{min}}^{0.83} d\tau \int_{\tau/0.83}^1 \frac{dx}{x} f_{\gamma/e}(\tau/x) f_{q/p}(x, Q^2) \hat{\sigma}(\tau s) \quad (12)$$

with  $\tau_{min} = (M_W + M_q)^2/s$

The sum of resolved and direct contribution, in principle, should not depend on value of the parameter  $\Lambda$ . The effects of  $\Lambda$  on the cross sections and contributions of direct and resolved parts are given in Table II. In Table III integrated total cross sections times branching ratio of  $W \rightarrow \mu\nu$  and corresponding number of events are shown for various values of  $\kappa$  and  $\lambda$ . Through the calculations proton structure functions of Martin, Robert and Stirling (MRS A) [19] and photon structure functions of Drees and Grassie (DG) [20] have been used with  $Q^2 = M_W^2$ . Here number of events has been calculated using

$$N = \sigma(\gamma p \rightarrow W + Jet) B(W \rightarrow \mu\nu) A L_{int} \quad (13)$$

where we take the acceptance in the muon channel A and integrated luminosity  $L_{int}$  as 65% and  $200\text{pb}^{-1}$ . To give an idea about the comparison with corresponding ep collider the cross sections obtained using Weizsäcker-Williams approximation are also shown on the same table. As the cross section  $\sigma(\gamma p \rightarrow W + Jet)$  we have considered the sum of  $\sigma(\gamma u \rightarrow W^+ d)$ ,  $\sigma(\gamma \bar{d} \rightarrow W^+ \bar{u})$ ,  $\sigma(\gamma \bar{s} \rightarrow W^+ \bar{c})$ ,  $\sigma(\gamma u \rightarrow W^+ s)$ ,  $\sigma(\gamma \bar{s} \rightarrow W^+ \bar{u})$ , and  $\sigma(\gamma \bar{d} \rightarrow W^+ \bar{c})$ . As shown from Table III the cross sections using backscattered laser photons are considerably larger than the case of corresponding ep collision. We assume that the form factor structure of  $\kappa - 1$  and  $\lambda$  do not depend on the momentum transfers at the energy region considered. Then anomalous terms containing  $\kappa$  grow with  $\sqrt{\hat{s}}/M_W$  and terms with  $\lambda$  rise with  $\hat{s}/M_W^2$ . Deviation  $\Delta\kappa = \kappa - 1 = 1$  from SM value changes the total cross sections 30-70% whereas the  $\Delta\lambda = \lambda = 1$  gives 80% changes. Therefore high energy will improve the sensitivity to

anomalous couplings. For comparison with HERA energy  $\sqrt{s} = 314$  GeV the similar results would be 20-40% for  $\Delta\kappa = 1$  and 5% for  $\Delta\lambda = 1$ .

TABLE II. Integrated total cross section times branching ratios  $\sigma(\gamma p \rightarrow Wj) \times B(W^+ \rightarrow \mu\nu)$  in pb to indicate direct and resolved photon contribution depending on invariant kinematical cut  $\Lambda$  in GeV. DG and MRS A were used for photon and proton structure functions.

$\kappa, \lambda$	$\sigma_{dir} \times B(W^+ \rightarrow \mu\nu)$		
	$\Lambda = 0.2$	$\Lambda = 1$	$\Lambda = 5$
1,0	12.12	11.34	10.57
1,1	23.43	22.66	21.88
1,2	57.37	56.59	55.82
0,0	8.08	7.31	6.53
2,0	21.70	20.92	20.14
	$\sigma_{res} \times B(W^+ \rightarrow \mu\nu)$		
	-0.77	0.92	2.62

TABLE III. Integrated total cross section times branching ratio  $\sigma(\gamma p \rightarrow Wj) \times B(W^+ \rightarrow \mu\nu)$  in pb and corresponding number of events(in parentheses) without cutoff for massive quarks. Integrated luminosity  $L_{int} = 200pb^{-1}$  has been used.

Backscattered Laser	WWA	$\kappa$	$\lambda$
13.8(1780)	1.3(170)	1	0
25.1(3262)	1.9(246)	1	1
59.0(7670)	3.7(480)	1	2
9.7(1262)	0.9(120)	0	0
23.4(3042)	2.1(274)	2	0

It is important to see how the anomalous couplings change the shape of the transverse momentum distributions of the final quark jet. For this reason we use the following formula:

$$\frac{d\sigma}{dp_T} = 2p_T \int_{y^-}^{y^+} dy \int_{x_a^{min}}^{0.83} dx_a f_{\gamma/e}(x_a) f_{q/p}(x_b, Q^2) \left( \frac{x_a x_b s}{x_a s - 2m_T E_p e^y} \right) \frac{d\hat{\sigma}}{d\hat{t}} \quad (14)$$

where

$$y^\mp = \log \left[ \frac{0.83s + m_q^2 - M_W^2}{4m_T E_p} \mp \left\{ \left( \frac{0.83s + m_q^2 - M_W^2}{4m_T E_p} \right)^2 - \frac{0.83E_e}{E_p} \right\}^{1/2} \right] \quad (15)$$

$$x_a^{(1)} = \frac{2m_T E_p e^y - m_q^2 + M_W^2}{s - 2m_T E_e e^{-y}}, \quad x_a^{(2)} = \frac{(M_W + m_q)^2}{s}$$

$$x_a^{min} = \text{MAX}(x_a^{(1)}, x_a^{(2)}), \quad x_b = \frac{2m_T E_e x_a e^{-y} - m_q^2 + M_W^2}{x_a s - 2m_T E_p e^y} \quad (16)$$

with

$$\hat{s} = x_a x_b, \quad \hat{t} = m_q^2 - 2E_e x_a m_T e^{-y}, \quad \hat{u} = m_q^2 + M_W^2 - \hat{s} - \hat{t}$$

$$m_T^2 = m_q^2 + p_T^2 \quad (17)$$

The  $p_T$  spectrum  $B(W \rightarrow \mu\nu) \times d\sigma/dp_T$  of the quark jet is shown in Fig. 1 for various  $\kappa$  and  $\lambda$  values at LC+HERAp based  $\gamma p$  collider. Similar distribution is given in Fig. 2 for Weizsäcker-Williams Approximation that covers the major contribution from ep collision. It is clear that the cross section at large  $p_T$  is quite sensitive to anomalous  $WW\gamma$  couplings. As  $\lambda$  increases the cross section grows more rapidly when compared with  $\kappa$  dependence at high  $p_T$  region  $p_T > 100$  GeV. The cross sections with real gamma beam are one order of magnitude larger than the case of WWA. Comparison between two figures also shows that the curves become more separable as  $\hat{s}$  gets large.

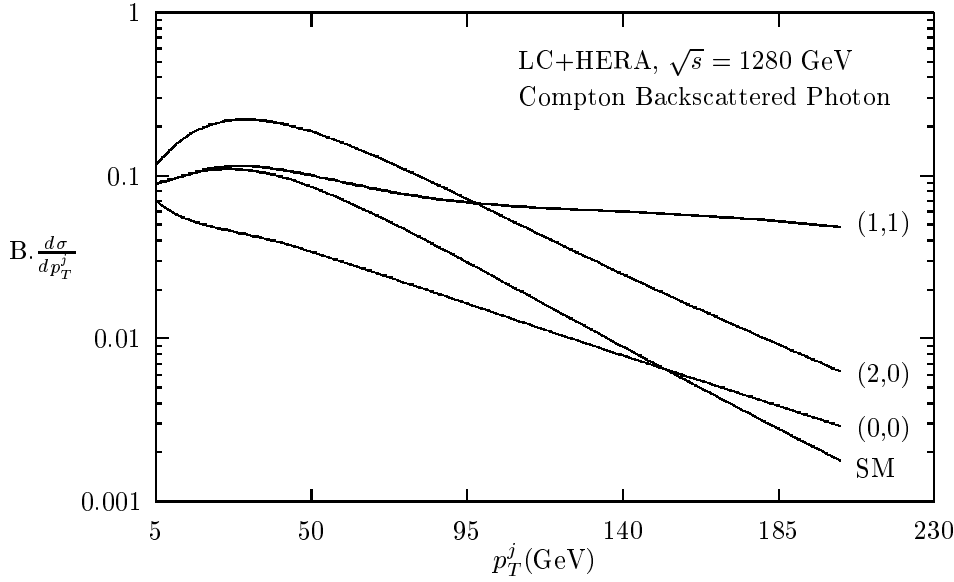


FIG. 1.  $\kappa$  and  $\lambda$  dependence of the transverse momentum distribution of the quark jet at LC+HERAp based  $\gamma p$  collider (Compton Backscattered Photon). The unit of the vertical axis is pb/GeV and the numbers in the parentheses stand for anomalous coupling parameters  $(\kappa, \lambda)$ .

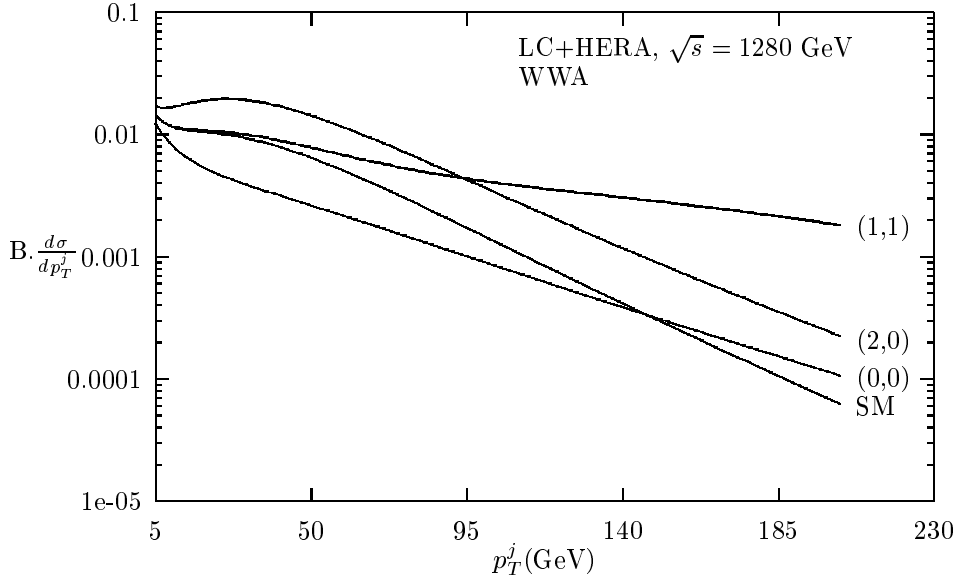


FIG. 2. The same as the Fig.1 but for Weizsäcker Williams Approximation.

### III. SENSITIVITY TO ANOMALOUS COUPLINGS

We can estimate sensitivity of LC+HERAp based  $\gamma p$  collider to anomalous couplings by assuming the 0.02 combined systematic error in the luminosity measurement and detector acceptance for the integrated luminosity value of  $200 \text{ pb}^{-1}$ . We use the simple  $\chi^2$ -criterion to obtain sensitivity as follows

$$\chi^2 = \sum_{i=\text{bins}} \left( \frac{X_i - Y_i}{\Delta_i^{exp}} \right)^2 \quad (18)$$

$$X_i = \int_{V_i}^{V_{i+1}} \frac{d\sigma^{SM}}{dV} dV, \quad Y_i = \int_{V_i}^{V_{i+1}} \frac{d\sigma^{NEW}}{dV} dV \quad (19)$$

$$\Delta_i^{exp} = X_i \sqrt{\delta_{stat}^2 + \delta_{sys}^2}, \quad V = p_T \quad (20)$$

We have divided  $p_T$  region of the final quark into equal pieces for binning procedure and have considered at least 10 events in each bin. For sensitivity, the number of  $W^+$  and  $W^-$  events given with their branching ratios in the  $\mu\nu$  and  $e\nu$  channels has been taken into account. Using the above formula the limits on the  $\Delta\kappa$  and  $\lambda$  are given in Table IV for the deviation of the cross section from the Standard Model value at 68% and 95% confidence levels with and without systematic error. On the ground of comparison we give the limits from ep collider in Table V using Weizsäcker-Williams approximation.

From these tables we see that  $\gamma p$  mode of LC+HERAp probes  $\Delta\kappa$  and  $\lambda$  with better sensitivity than present colliders and comparable with LHC in the case of  $\Delta\kappa$  but worse than linear  $e^-e^+$  collider. The advantage of the process  $\gamma p \rightarrow Wj$  is that it probes the  $WW\gamma$  couplings independently of  $WWZ$  effects. After further improvement of energy and luminosity, linac-ring type  $\gamma p$  collider possibly will give complementary information to LHC and LC.

TABLE IV. Sensitivity of LC+HERAp based  $\gamma p$  collider to anomalous couplings for real photons.  $L_{int} = 200pb^{-1}$ . Only one of the couplings is assumed to deviate from the SM at a time.

Sys. error	68%C.L.	68%C.L.
$\delta^{sys} = 0$	$-0.019 < \Delta\kappa < 0.019$	$-0.075 < \lambda < 0.075$
$\delta^{sys} = 0.02$	$-0.022 < \Delta\kappa < 0.022$	$-0.078 < \lambda < 0.078$
	95%C.L.	95%C.L.
$\delta^{sys} = 0$	$-0.038 < \Delta\kappa < 0.037$	$-0.11 < \lambda < 0.11$
$\delta^{sys} = 0.02$	$-0.044 < \Delta\kappa < 0.042$	$-0.11 < \lambda < 0.11$

TABLE V. Sensitivity of LC+HERAp collider to anomalous couplings for WWA.  $L_{int} = 200pb^{-1}$ .

Sys. error	68%C.L.	68%C.L.
$\delta^{sys} = 0$	$-0.068 < \Delta\kappa < 0.066$	$-0.28 < \lambda < 0.28$
$\delta^{sys} = 0.02$	$-0.069 < \Delta\kappa < 0.067$	$-0.28 < \lambda < 0.28$
	95%C.L.	95%C.L.
$\delta^{sys} = 0$	$-0.14 < \Delta\kappa < 0.13$	$-0.39 < \lambda < 0.39$
$\delta^{sys} = 0.02$	$-0.14 < \Delta\kappa < 0.13$	$-0.39 < \lambda < 0.39$

## ACKNOWLEDGMENTS

Authors are grateful to the members of the AUHEP group and S. Sultansoy for drawing our attention to anomalous couplings.

---

- [1] DELPHI Collaboration, P. Abreu *et al.*, CERN-EP/99-62 (1999)(to be published in Phys. Lett. B).
- [2] D0 Collaboration, B. Abbot *et al.* Phys. Rev. **D60**, 072002 (1999).
- [3] M.N. Dubinin and H.S. Song, Phys. Rev. **D57**, 2927 (1998).
- [4] U. Baur, J. Vermaseren and D. Zeppenfeld, Nucl. Phys. **B375**, 3 (1992)
- [5] C.S. Kim, Jungil Lee and H.G. Song, Z. Phys. **C63**, 673 (1994).
- [6] U. Baur and D. Zeppenfeld, Nucl. Phys. **B325**, 253 (1989).
- [7] M. Janssen, Z. Phys. **C52**, 165, 1991; M. Böhm and A. Rosado, *ibid.* **39**, 275 (1988).
- [8] V.A. Noyes, Proceedings of the Workshop on Future Physics at HERA 1995/96, edited by Ingelman, a. De Roeck and R. Klanner, p. 190; S. Godfrey, Z. Phys. **C55**, 619, 1992; T. Helbig and H. Spiesberger, Nucl. Phys. **B373**, 73 (1992); U. Baur and M.A. Doncheski, Phys. Rev. **D46** 1959 (1992).
- [9] ATLAS Technical Design Report Vol. II 1999.
- [10] Conceptual Design Report of LC500, DESY 1997-048.
- [11] D. Trines, Proceedings of the International Workshop on the Linac-Ring Type ep and  $\gamma p$  Colliders, published in Turkish J. Phys. **22**, 529 (1998).
- [12] R. Brinkmann, *ibid.*, **22**, 661 (1998); Z.Z. Aydin, A.K. Ciftci and S. Sultansoy, Nucl. Instrum. and Meth. **A351**, 261 (1994).
- [13] A. De Roeck, Turkish J. Phys. **22**, 595 (1998).
- [14] S.I. Alekhin *et al.*, Int. J. Mod. Phys. **A6**, 21 (1991); A.K. Ciftci, S. Sultansoy, S. Turkoz and O. Yavas, Nucl. Instrum. and Meth. **A365**, 317 (1995); A.K. Ciftci, Turkish J. Phys. **22**, 675 (1998).
- [15] Z.Z. Aydin *et al.*, Int. J. Mod. Phys. **A11**, 2019 (1996).
- [16] S. Atag and O. Cakir, Phys. Rev. **D49** 5769 (1994); O. Cakir and S. Atag, J. Phys. **G21** 1189 (1995); S. Atag, A. Celikel and S. Sultansoy, Phys. Lett. **B326** 185 (1994); A.T. Alan, Z.Z. Aydin and S. Sultansoy, Phys. Lett. **B327** 70 (1994); A.T. Alan, S. Atag and Z.Z. Aydin, J. Phys. **G20** 1399 (1994); A. Kandemir and U. Yilmazer, Phys. Lett. **B385** 143 (1996).
- [17] K.J.F. Gaemers and G.J. Gounaris, Z. Phys. **C1**, 259 (1979).
- [18] K. Hagiwara, R.D. Peccei, D. Zeppenfeld and K. Hikasa, Nucl. Phys. **B282**, 253 (1987).
- [19] A.D. Martin, W.J. Stirling and R.G. Roberts, Phys. Rev. **D51**, 4756 (1995).
- [20] M. Drees and K. Grassie, Z. Phys. **C28** 451 (1985).